

**Morphological and biochemical changes in *Phaeodactylum tricornutum* triggered by culture media: Implications for industrial exploitation**

Zhongdi Song <sup>a</sup>, Gary J Lye <sup>a</sup>, Brenda M Parker <sup>a,\*</sup>

<sup>a</sup> The Advanced Centre for Biochemical Engineering, Department of Biochemical Engineering, University College London, London, WC1E 6BT, United Kingdom

\*Corresponding author: Brenda M Parker

Tel.: +44(0)20 7679 9789.

E-mail address: [brenda.parker@ucl.ac.uk](mailto:brenda.parker@ucl.ac.uk)

E-mail address: [zhongdi.song.15@ucl.ac.uk](mailto:zhongdi.song.15@ucl.ac.uk) (Zhongdi Song)

[g.lye@ucl.ac.uk](mailto:g.lye@ucl.ac.uk) (Gary J Lye)

Declarations of interest: none

Abbreviations: EST, expressed sequence tag; EPS, exopolysaccharides; DW, dry weight; FAME, fatty acid methyl ester; NL, neutral lipid; PL, polar lipid; TFA, total fatty acid; TAG, triacylglyceride; SFA, saturated fatty acid; MUFA, monounsaturated fatty acid; PUFA, polyunsaturated fatty acid; EPA, eicosapentaenoic acid; DHA, docosahexaenoic acid; DMF, *N,N*-dimethylformamide; PMSF, phenylmethylsulfonyl fluoride; PSA, phenol sulphuric acid; M & M medium, Mann and Myers' medium; SQDG, sulfoquinovosyl diacylglycerol; RP-HPLC, reverse phase high-performance liquid chromatography; PTFE, polytetrafluoroethylene; AFA, adaptive focused acoustics.

## Abstract

*Phaeodactylum tricornutum* is a polymorphic marine diatom, displaying three main morphotypes: fusiform, triradiate and oval. It is of great interest for industrial biotechnology as a natural rich source of valuable eicosapentaenoic acid (EPA) and fucoxanthin. Changing culture conditions such as temperature and salinity has been shown to elicit morphological changes in *P. tricornutum*. However, limited information is available about the conditions that can be used for controlling cell morphology and growth of a particular cell morphotype with high biomass productivity. While the phenomenon of pleiomorphy is intrinsically interesting, there has not been a systematic study linking this behavior to the ability of *P. tricornutum* to perform as a platform for industrial biotechnology. In this study, the effects of culture medium and culture age on morphological and biochemical changes in *P. tricornutum* were investigated. Mann and Myers' medium was identified as eliciting significant morphotype conversion from fusiform to oval in *P. tricornutum*. Liquid cultures containing more than 90% oval cells were obtained and well-maintained in this medium under constant shaking condition, allowing high dry biomass concentration ( $0.73 \text{ g L}^{-1}$ ) to be achieved. Biochemical composition analyses revealed that higher protein (% dry weight) was obtained from oval cell cultures compared to fusiform cell cultures maintained in f/2 medium over 21 days cultivation. Meanwhile, pigment was markedly accumulated in oval cell cultures whereas lipid and carbohydrate were highly accumulated in fusiform cell cultures. This work offered a novel way to regulate cell morphology of *P. tricornutum* and provided significant implications for upstream cultivation strategies to optimise manufacture of different classes of product in *P. tricornutum*.

**Keywords:** *Phaeodactylum tricornutum*, pleiomorphy, biochemical composition, culture

medium, biorefining

## 1. Introduction

*Phaeodactylum tricornutum* is a pennate diatom (Heterokonta) that has been extensively studied as a model system for diatom biology, physiology and ecology. Its genome has been sequenced [1] and a diatom expressed sequence tag (EST) database containing 130,000 *P. tricornutum* ESTs has been constructed [2]. *P. tricornutum* grows in brackish to saline water with a high growth rate of  $0.09 \text{ h}^{-1}$  under optimal conditions [3]. This species is a rich source of the high-value omega-3 fatty acid eicosapentaenoic acid (EPA), and the marine carotenoid fucoxanthin [4, 5]. EPA is essential for brain and eye development of infants and has been shown to prevent or reduce the risk of some diseases, such as cardiac disease, inflammation and cancers [6, 7]. Fucoxanthin has also been found to have multiple bioactivities including antioxidant, anti-cancer, anti-inflammatory, anti-obesity and anti-diabetic effects [8]. Additionally, *P. tricornutum* is considered as a potential renewable feedstock for biofuels production due to its capability to accumulate high lipids and carbohydrates, particularly under nitrogen starvation [9].

*P. tricornutum* has a unique property of polymorphism, displaying three main morphotypes: fusiform, triradiate and oval [10]. Unlike typical diatoms, the cell wall of *P. tricornutum* is poorly silicified [11], which may be an advantage for *P. tricornutum* biotechnology in terms of intracellular product recovery during bioprocessing, compared to other diatoms with rigid cell walls. The fusiform and triradiate types are better adapted to the planktonic lifestyle whereas the oval form tends to be benthic, having a higher sedimentation rate [12]. Furthermore, oval cells possess a raphe and can secrete mucilaginous exopolymeric substances, favoring gliding motility and cell adhesion [12, 13].

*P. tricornutum* has been shown to undergo cell morphological conversions in response to

fluctuations in growth conditions such as salinity, temperature and pH. Ten strains of *P. tricornutum* (Pt1-Pt10) isolated from different geographic locations worldwide were characterised genetically and phenotypically [14]. Another strain Pt1 8.6 is one monoclonal culture derived from Pt1 and has been selected for genome sequencing [1]. Among these strains, the fusiform morphotype was found to be most stable and frequently observed in cell cultures. However, significant cell morphotype change from fusiform to oval occurred in strains Pt1 8.6, Pt3 and Pt9, induced by low temperature (15 °C) or hyposaline conditions [12, 14]. Enrichment of oval cells could also be achieved through successive transfers on solid medium [15, 16]. Under these suboptimal conditions, despite the significant conversion in cell morphotype, the overall cell growth rate and biomass productivity experienced an evident decrease [12], which is not beneficial for industrial applications. Other unfavourable conditions such as nutrient limitation, low light intensity, red light and low calcium concentration ( $< 15 \text{ mg L}^{-1}$ ) were reported to promote oval cell production as well, but the changes in cell morphotype were not significant or the results still need verification [11, 14, 17, 18]. Triradiate cells are rarely observed in laboratory cultures except for the strain Pt8 [14], though high pH or high dissolved inorganic carbon were reported to increase their abundance [19]. Despite these observations, limited information is available about the conditions that can be used for controlling cell morphology and maintenance of each cell morphotype of *P. tricornutum*.

Cell morphology and biochemical profiles reflect the physiological and metabolic status of cells under the specific growth conditions. Although product accumulation in *P. tricornutum* cells has been characterised under diverse culture conditions, few studies quantify the proportion of cell morphotypes. Little is therefore known about the biochemical differences

between the cell morphotypes.

While the phenomenon of pleiomorphy is intrinsically interesting, there has not been a systematic study linking this behavior to the ability of *P. tricornutum* to perform as a platform for industrial biotechnology. In this study, a culture medium triggering significant cell morphotype conversion in *P. tricornutum* from fusiform to oval and suitable for maintenance of oval cells in liquid cultures was identified. This enabled biochemical profiles in both morphotypes to be investigated in support of their further industrial exploitation.

## **2. Materials and Methods**

### **2.1 Strains and cultivation conditions**

*Phaeodactylum tricornutum* strains Pt1 8.6 (CCAP 1055/1) and Pt4 (CCAP 1052/6) were acquired from the Culture Collection of Algae and Protozoa (CCAP, UK). Stock cultures were maintained in f/2-enriched artificial seawater made from Instant Ocean salt (Instant Ocean, UK) [20] (Table S1). As *P. tricornutum* is facultative for silicate, it was not added in this study. All cultures were grown at 20 °C with 100 rpm shaking under continuous light illumination at 80  $\mu\text{mol photons m}^{-2} \text{s}^{-1}$  from fluorescent lamps (P0300-0221, GroLux T8 15W Sylvania, Eppendorf, UK) factory-installed in the shaker (New Brunswick™ Innova® 44, Eppendorf, UK).

### **2.2 Cell morphological changes study**

Experimental cultures were grown in either f/2 medium or Mann and Myers' medium (hereafter M & M medium) [21] (Table S1). Log-phase cultures of Pt1 8.6 and Pt4 grown in f/2 medium were centrifuged at 4000 rpm for 10 min and transferred to fresh f/2 medium or M & M medium to pre-acclimate for 6 days (denoted as the 1st transfer). The pre-acclimated cultures were then inoculated in 250 mL Erlenmeyer flasks containing 100 mL of respective

culture medium with an initial cell density of  $8-10 \times 10^5$  cells  $\text{mL}^{-1}$  (denoted as the 2nd transfer). Subculturing treatments denoted as the 3rd, 4th and 5th transfer were conducted when it was estimated that late stationary phase was reached ( $\sim$ day 21), giving an initial cell density as above. Morphological studies were performed in biological duplicates. The relative proportions of fusiform, oval and triradiate morphotypes in cultures were determined using a haemocytometer. A minimum of 500 cells were counted per replica.

### **2.3 Cultivation for growth and biochemical analyses**

The pleiomorphic property of *P. tricornutum* motivated us to investigate other characteristics such as growth kinetics and biochemical profiles including pigment, protein, fatty acid and carbohydrate of various cell morphotypes. After six transfers representing a cell cultivation of more than four months, the well-maintained log-phase cultures of Pt1 8.6 and Pt4 grown in the two media were inoculated in 250 mL Erlenmeyer flasks containing 100 mL of respective culture medium with an initial cell density of  $8-10 \times 10^5$  cells  $\text{mL}^{-1}$ . Cultures were monitored for 21 days for growth measurement and 1 mL or 2 mL samples were taken on day 3, 7, 10, 14 and 21 for pigment analysis. For protein, carbohydrate and lipid analyses, experimental cultures were prepared in 500 mL Pyrex glass flasks containing 200 mL of respective culture medium. Samples were harvested on day 3, 8, 14 and 21 by centrifugation and stored at  $-80$  °C until for further biochemical analyses. Growth and biochemical analyses were conducted in biological triplicates.

### **2.4 Cell growth and dry biomass determination**

The growth of *P. tricornutum* cells maintained in the two culture media was determined by cell counting. The specific growth rate ( $k$ ) is calculated with the equation:  $k = (\ln N_2 - \ln N_1) / (t_2 - t_1)$ , where  $N$  is the cell density ( $\text{mL}^{-1}$ ) and  $t$  is the time after inoculation (d) at time 1 and 2

respectively. Dry biomass concentration ( $\text{g L}^{-1}$ ) was measured as follows. Culture samples (10-20 mL) were centrifuged at 4000 rpm for 15 min, washed with distilled water and then resuspended in a small volume of distilled water. Cell suspensions were filtered through pre-weighed GF/C glass microfiber filters (Whatman, GE Healthcare Life Sciences) and dried in an oven at 80 °C until a constant mass was achieved.

## **2.5 Biochemical composition characterisation**

### **2.5.1 Pigment analysis**

The pigment composition and content in *P. tricornutum* were analysed by a reverse phase high-performance liquid chromatography (RP-HPLC) method. Pigment was extracted based on the EnAlgae protocol [22]. Briefly, *P. tricornutum* cells were incubated in 1 ml of *N,N*-dimethylformamide (DMF) at 250 rpm for 15 min at room temperature. Following centrifugation at 15000 rpm for 5 min, the extracts were collected and filtered through 0.2  $\mu\text{m}$  polytetrafluoroethylene (PTFE) syringe filters. All extraction procedures were performed under dimmed light to avoid light-induced degradation of pigments. The filtered pigment extracts were injected into a Dionex UltiMate 3000 HPLC system (Dionex, UK). Separation was performed in an ACE 5 C18 column (150 mm x 4.6 mm, 5  $\mu\text{m}$  particle size, Advanced Chromatography Technologies Ltd, UK). The mobile phase was pumped in at a flow rate of 1  $\text{mL min}^{-1}$  programmed as follows: an initial 4 min linear gradient from 100% solvent A (80% (v/v) methanol containing 0.5 M ammonium acetate, pH 7.2) to 100% solvent B (90% (v/v) acetonitrile), followed by a linear gradient to 20% solvent B and 80% solvent C (100% ethyl acetate) in 14 min. The column was returned to initial conditions by a 3 min linear gradient to 100% solvent B and another 3 min linear gradient to 100% solvent A and then re-equilibrated in 100% solvent A for 5 min before the next injection [23]. The eluted pigments

were detected at 440 nm using a diode array detector and identified by co-elution with a mixed pigments standard (PPS-MIX-1, DHI, Denmark). Quantitative analysis was achieved through calibration curves created from each individual standard (DHI, Denmark).

### **2.5.2 Total soluble protein determination**

*P. tricornutum* cells (~1.5 mg dry biomass) were resuspended in 1 mL of chilled lysis buffer made of 50 mM Tris-HCl pH 8.0, 10 mM EDTA, 0.1% (v/v) TritonX-100 and 0.5 mM phenylmethylsulfonylfluoride (PMSF). Cell suspensions were transferred into 1 mL millitubes with AFA (adaptive focused acoustics) fibres (Covaris, UK) and subjected to focused acoustic disruption using a Covaris E210 Focused-ultrasonicator (Covaris, UK). The operation conditions are cycles per burst: 1000, intensity (mv): 10, duty factor (%): 20 and water bath: 10 °C. Treatment time employed was depending on the cell morphotype, achieving a cell disruption efficiency of more than 97%. Cell debris was removed by centrifugation at 15000 rpm for 20 min at 4 °C. The total soluble protein content was determined using the Coomassie (Bradford) Protein Assay kit (No. 23200, Thermo Scientific) with bovine serum albumin as a standard.

### **2.5.3 Carbohydrate determination**

Two carbohydrate fractions including exopolysaccharides (EPS) and cellular carbohydrate were determined according to the method described previously [24] and the modified EnAlgae protocol. Cell broth was centrifuged at 4000 rpm for 15 min. 6-10 mL of the supernatant was transferred to a new Falcon tube for EPS precipitation by adding 3 volumes of chilled ethanol and incubating at 4 °C overnight. The precipitated EPS was resuspended in 1 mL of MilliQ water and analysed for carbohydrate using the phenol sulphuric acid (PSA) assay [25]. Cell pellets (~1.5 mg dry biomass) were resuspended in 1 mL of MilliQ water and

transferred into 1 mL millitubes for focused-ultrasonication. The samples were then transferred to glass test tubes containing 1 mL of 1 M sulphuric acid, mixed thoroughly, and incubated at 90 °C for 1 h. Following centrifugation at 15000 rpm for 10 min, the supernatants were measured for cellular carbohydrate with the PSA assay.

The cellular carbohydrate extracts were further analysed by high-performance anion-exchange chromatography (HPAEC) after hydrolysis in 0.5 M sulphuric acid for 1 h at 121 °C in an autoclave [26]. Monosaccharide separation was achieved using a Dionex ICS 5000<sup>+</sup> system equipped with an AminoPac PA10 column (250 mm x 4 mm, Dionex, UK) and a pulsed amperometric detector following the procedure of an isocratic elution of 1 mM KOH for 25 min at 0.25 mL min<sup>-1</sup>. Standards (glucose, galactose, mannose, etc.) used for identification and quantification were obtained from Sigma-Aldrich.

#### **2.5.4 Neutral lipid and fatty acid analysis**

Neutral lipids were qualitatively detected through BODIPY 505/515 cell staining [27]. Aliquots of a BODIPY 505/515 (D3921, Invitrogen) stock solution dissolved in dimethyl sulfoxide (DMSO) were added directly to 1 mL of cell suspensions ( $\sim 2 \times 10^6$  cells mL<sup>-1</sup>) to achieve a final dye concentration of 1  $\mu\text{g mL}^{-1}$ . Each sample was mixed and incubated in darkness for 10 min at room temperature. Fluorescent images of lipid bodies were made using an epifluorescence microscope (TE2000-U, Nikon, Japan) with filter blocks of excitation set from 450 to 490 nm and emission set from 500 to 550 nm. Bright-field images were made simultaneously under phase contrast.

Fatty acid detection was performed following the procedure of lipid extraction, transesterification and gas chromatography (GC) analysis using the modified EnAlgae protocol. Lipid was extracted from cell pellets ( $\sim 3$  mg dry biomass) by adding 8 mL of a

chloroform:methanol (2:1, v/v) mixture. Pentadecanoic acid (200 µg) was added as an internal standard. After sonicated for 30 min and incubated for another 30 min in an iced bath, 2 mL of deionized water was added to form two separate phases. The lower phase containing lipids was recovered, evaporated and resuspended in 200 µL of n-heptane. Transesterification was performed by adding 3 mL of methanol containing 2.5% (v/v) H<sub>2</sub>SO<sub>4</sub> into 60 µL of lipid extracts and incubating at 60 °C for 4 h. The fatty acid methyl esters (FAMES) were analysed on a Trace 1300 gas chromatograph (Thermo Scientific, UK) equipped with an Rxi-5Sil MS column (30 m × 0.25 mm, 0.5 µm film thickness, Restek, UK) and a flame ionisation detector (FID). Helium was used as the carrier gas at a flow rate of 1.2 mL min<sup>-1</sup>. Injector and detector temperatures were set at 230 °C and 250 °C, respectively. The oven temperature was programmed as follows: 80 °C for 2 min, to 180 °C at 15 °C min<sup>-1</sup> and to 240 °C at 2.5 °C min<sup>-1</sup>, hold for 10 min. FAMES were identified by co-elution with a FAME standard mix (Supelco 37 Component FAME Mix, Sigma Aldrich) and quantified from calibration curves of external standards (methyl esters of C<sub>14:0</sub>, C<sub>16:0</sub>, C<sub>16:1</sub>, etc., Sigma-Aldrich). All FAME concentrations were normalised against the methyl pentadecanoate from the internal standard. Total FAME content was calculated as the sum of all individual FAMES.

## **2.6 Statistical analysis**

Statistical analyses were performed using Student's t-test in Microsoft Office Excel 2007 (Microsoft, Redmond, Washington, USA). Data were considered significantly different at the level of  $p < 0.05$ .

## **3. Results and Discussion**

### **3.1 Morphological response of *P. tricornutum* to different culture media**

As *P. tricornutum* is pleiomorphic, it may be important to be able to selectively control growth of a particular morphotype for a particular industrial application. Two previously reported culture media, f/2 medium and M & M medium, were chosen for *P. tricornutum* cultivation in order to determine if changes in medium composition will influence cell morphology of *P. tricornutum*. Upon arrival from CCAP, the genome sequenced strain Pt1 8.6 consisted of approximately 88% fusiform, 10% triradiate and less than 3% oval cells, and another strain Pt4, possessing a different genotype from Pt1 8.6, contained mainly the fusiform morphotype (~ 97% fusiform, 3% oval and <0.5% triradiate). Cultivation for 30 days in f/2 medium did not significantly change the morphotype abundance in either strain, showing stability for many cell divisions (Figure 1A). Contrastingly, when cells were transferred and grown for 30 days in M & M medium, a marked increase in the abundance of oval cells from 2.9% to 38.4% in Pt1 8.6 and from 5.7% to 18.4% in Pt4 with a corresponding decrease in fusiform (from 91.3% to 58.5% in Pt1 8.6 and from 93.9% to 81.6% in Pt4) and triradiate morphotypes was observed gradually over time (Figure 1A). These results suggested that the oval morphotype was preferred by *P. tricornutum* as a response and an adaption to the M & M medium and confirmed that cell morphological transformation could be triggered by changing growth conditions.

Successive transfers on solid medium were found to enrich oval cells in Pt2 [15]. In this study, oval cells were also enriched in M & M medium after five subculturing treatments. In contrast to Pt4, the fusiform and triradiate cells did not disappear entirely in Pt1 8.6 cultures maintained in M & M medium. After four months, 90.8% of cells were oval in Pt1 8.6 cultures and almost all the cells (99.9%) were oval in Pt4 cultures (Figure 1B). Microscopic images clearly showed the fusiform and oval morphotypes in two strains maintained in f/2

medium or M & M medium (Figure 1C). This new cell morphotype abundance obtained in both strains remained stable during subsequent passages in M & M medium.

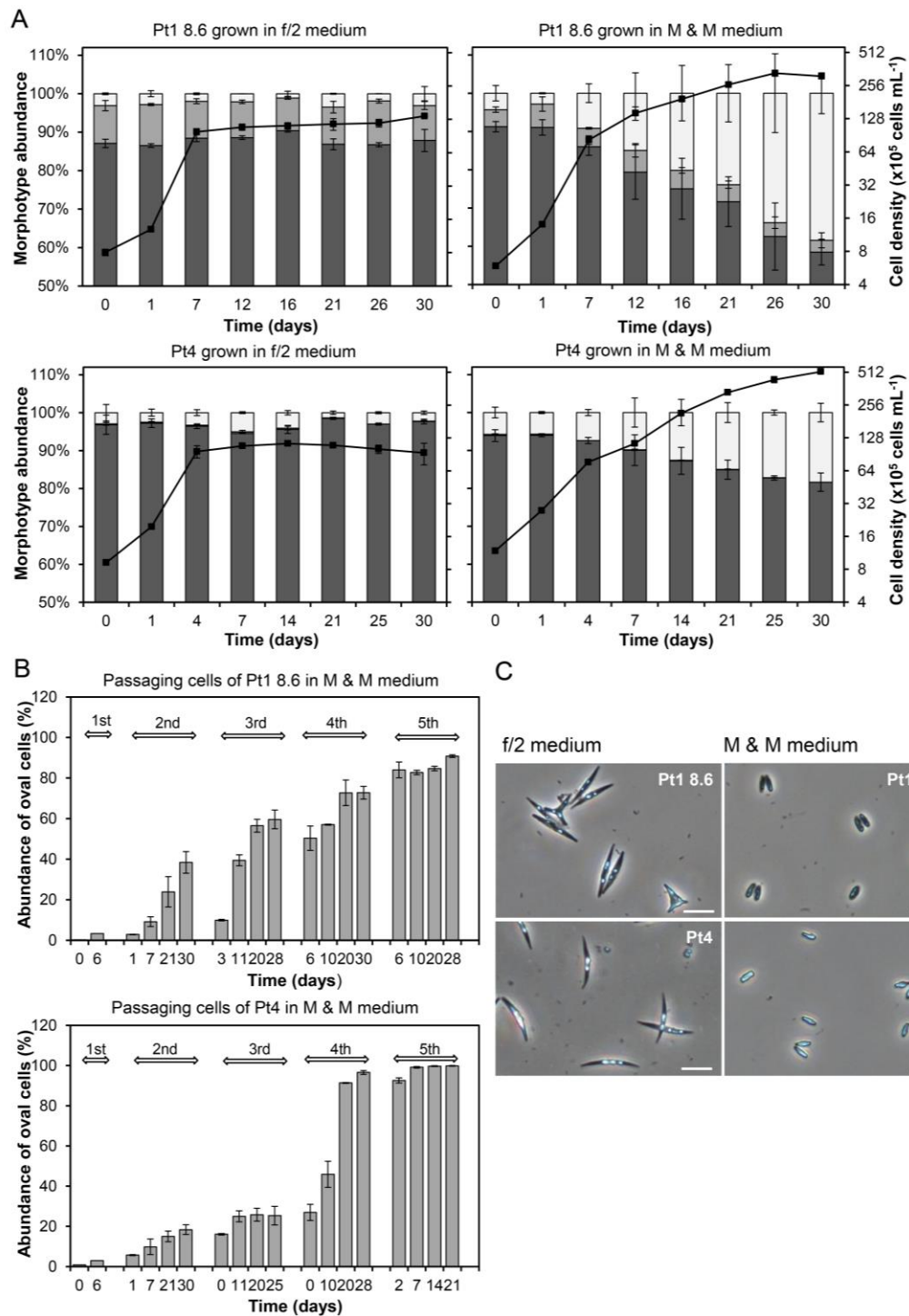


**Figure 1** Effects of culture media on cell morphology and growth of two *P. tricornutum* strains. (A) Relative abundance of fusiform (dark grey bars), triradiate (light grey bars) and

oval cells (white bars) in Pt1 8.6 and Pt4 cultures maintained in f/2 medium and after a transfer from f/2 medium to M & M medium (with a pre-acclimation to M & M medium for 6 days). Growth curves of total cells are represented by solid lines. (B) Relative abundance of oval cells in Pt1 8.6 and Pt4 cultures during five successive transfers in fresh M & M medium. Data are shown as mean  $\pm$  one standard deviation from two biological replicates (n=2). (C) Micrographs showing representative examples of different cell morphotypes of Pt1 8.6 and Pt4 maintained in f/2 medium or M & M medium. Samples for imaging were taken from cultures after the fifth transfer. Scale bars: 20  $\mu$ m.

It has been demonstrated previously that the transformation of *P. tricornutum* cells between different morphotypes could be reversible [12, 15]. Thus, the obtained stable oval cell cultures maintained in M & M medium were centrifuged and inoculated back into the f/2 medium. A gradually reversible conversion from oval to fusiform was observed in Pt1 8.6 cultures. However, for Pt4, cell cultures displayed severe cell aggregation and the majority of cells existed still in the oval form even after several subculturing treatments (Figure S1). This indicated that under the tested conditions, the morphological conversion induced by M & M medium was reversible in Pt1 8.6 and might be irreversible in Pt4. It also further suggests that the mechanisms employed by cells for morphological changes may differ between genotype A of Pt1 8.6 and genotype B of Pt4 [14].

M & M medium has been used previously for *P. tricornutum* cultivation [4, 28]. However, the fact that this culture medium-triggered cell morphological change from fusiform to oval was first reported in this study and the specific factors capable of initiating oval cell production remain unknown. We carried out a preliminary investigation for rapid assessment of the impacts of medium components on cell morphology of *P. tricornutum*. The f/2 medium was

modified based on the nutrient components of M & M medium. Cultivation for 35 days in modified f/2 media showed that low salinity, high concentration of nitrate or phosphate, addition of Tris, M & M trace elements or omission of vitamins did not trigger significant cell morphotype change in both Pt1 8.6 and Pt4, with the fusiform morphotype being predominant (>90%) in cultures through microscopic examination (Figure S2).

Hyposaline conditions were reported to induce significant cell morphotype change to the oval form in Pt1 8.6 and Pt3. However, under low salinity (3.8 g L<sup>-1</sup>, 10sw), the proportion of oval cells was less than 10% in Pt1 8.6 on day 30 [12], much lower than the 38% obtained here in M & M medium. Furthermore, under hyposaline conditions, no evident morphotype conversion was found in Pt6 and Pt7 possessing the genotype D [11, 14]. These studies suggest that low salinity of M & M medium might be a contributing factor to the observed morphotype change in Pt1 8.6 but not the main one. There have been several studies focusing on the impact of nitrate concentration on *P. tricornutum* cells [9, 29]. Consistent with our observations, no cell shape change was reported under high nitrate concentrations.

It is commonly reported that cells tend to convert to oval type under stress conditions such as nutrient limitation [14]. Compared with f/2 medium, although the M & M medium contains more than 13-fold higher concentrations of nitrate and phosphate, it has lower Ca, Mg, Fe, Co and Cu content (Table S1). Therefore, it could be the balance of all nutrients which is important. Under relatively high nitrate and phosphate conditions, other nutrients such as Fe, Cu, Ca and Mg might become limited, which could be responsible for the observed phenomena. Furthermore, addition of Tris to f/2 medium was shown to have a negative effect on *P. tricornutum*, leading to severe cell aggregation in Pt1 8.6 and a slight decrease in biomass yield in Pt4 (Figure S2&S3), despite that no significant cell morphotype

change was observed under this tested condition. Further studies are required to elucidate the specific inducing factors to the observed cell morphotype conversions in *P. tricornutum* induced by M & M medium and to confirm the universality of this method in other *P. tricornutum* strains.

### **3.2 Growth and dry biomass of fusiform and oval *P. tricornutum* cells**

Fusiform cells are dominant in cultures grown in f/2 medium (denoted as fusiform cell cultures) whereas the oval form is the most abundant in cultures maintained in M & M medium (denoted as oval cell cultures). From a bioprocessing perspective, it is important to be able to quantify cell growth rate and dry biomass yield with regard to bioprocess design and scale-up. Consequently, we investigated the effects of culture medium on growth and biomass production of the two obtained cell morphotypes.

As shown in Figure 2A, similar growth rates for fusiform and oval cell cultures of Pt1 8.6 were obtained, with the maximum specific growth rates of  $0.68 \text{ d}^{-1}$  and  $0.70 \text{ d}^{-1}$ , corresponding to doubling times of 1.03 d and 0.99 d, respectively (Table S2). Fusiform cell cultures entered stationary phase from day 10, reaching a final cell density of approximately  $120 \times 10^5 \text{ cells mL}^{-1}$ . In contrast, oval cell cultures experienced a longer lag phase, kept growing after 10 days cultivation and appeared to only reach the early stationary phase on day 21, where a 3-fold higher cell density of  $374 \times 10^5 \text{ cells mL}^{-1}$  was achieved. Similar growth patterns were observed in Pt4 cultures except that a higher maximum specific growth rate was obtained for fusiform cell cultures compared to oval cell cultures ( $0.76 \text{ d}^{-1}$  versus  $0.43 \text{ d}^{-1}$ ; doubling time, 0.92 d versus 1.65 d) (Table S2). This is in agreement with the reported slower growth rate for the oval strain (Pt3) in comparison to fusiform strains and the doubling times obtained here were similar to those reported previously [14].

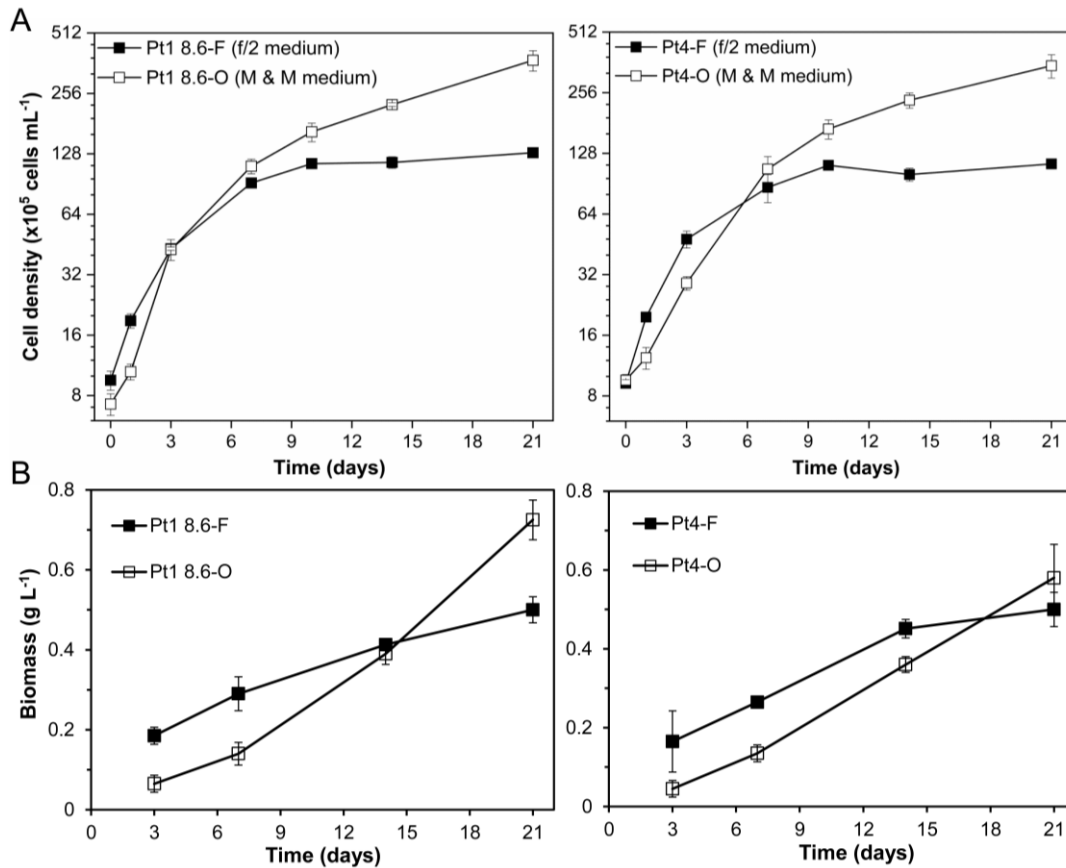


**Figure 2 Growth profiles of fusiform and oval *P. tricornutum* cultures maintained in two different culture media.** (A) Growth curves and (B) dry biomass concentration for fusiform (F) cell dominant cultures grown in f/2 medium or oval (O) cell dominant cultures grown in M & M medium in Pt1 8.6 and Pt4. Data are shown as mean  $\pm$  one standard deviation from three biological replicates (n=3).

Dry biomass yields over three weeks cultivation were also monitored for two cell morphotypes (Figure 2B). The highest biomass concentrations were obtained for oval cell cultures (0.73 g L<sup>-1</sup> in Pt1 8.6 and 0.58 g L<sup>-1</sup> in Pt4), compared to the 0.50 g L<sup>-1</sup> obtained for fusiform cell cultures of the two strains. The evident longer growth phase and markedly higher final cell and biomass concentrations for oval cell cultures could be attributed to the higher macronutrient content in M & M medium when compared to f/2 medium used to grow fusiform cells. However, from day 7 to day 14, oval cell cultures displayed lower

biomass concentrations despite higher total cell numbers than fusiform cell cultures (Figure 2). This could be explained by the smaller cell size of oval morphotype (~10  $\mu\text{m}$ ) than fusiform morphotype (~30  $\mu\text{m}$ ) as well as the differences in biomass composition between them. It has been shown that the percentages of nitrate and phosphate remaining in f/2 medium were approximately 0% after 7 days cultivation of *P. tricornutum*, which exhibited a similar growth pattern as our results observed for fusiform cell cultures [30]. Nutrient deprivation in f/2 medium at the stationary phase might therefore inhibit the growth of fusiform cells. In addition, a 5-fold increase in the dry biomass concentration from 0.5  $\text{g L}^{-1}$  to 2.5  $\text{g L}^{-1}$  was observed for *P. tricornutum* grown for 7 days in M & M medium when the  $\text{CO}_2$  concentration in the air supply increased from 0% to 1% [4]. From growth curves, stationary phase was not reached for oval cells even after 21 days cultivation (Figure 2). This implies that carbon might be an important limiting factor for fast growth of oval cells and further optimisation of cultivation parameters such as inorganic carbon supply may further increase growth rate and biomass production of oval *P. tricornutum* cells.

### **3.3 Biochemical responses of two cell morphotypes to different culture media**

#### **3.3.1 Pigment content and composition in fusiform and oval *P. tricornutum* cells**

Pigments, particularly fucoxanthin, represent a potentially valuable product from *P. tricornutum*, hence it is essential to determine types of pigment produced and their concentrations. The effects of culture time and culture medium on pigment content and composition in the two morphotypes of cells were studied and the pigment content was calculated on a dry weight (DW) basis in order to estimate specific yields and productivities.

Five major diatom pigments including chlorophyll *c*2 (Chl *c*2), fucoxanthin (Fuc), diadinoxanthin (Diad), chlorophyll *a* (Chl *a*) and  $\beta$ -carotene ( $\beta$ -car) were detected in fusiform

and oval *P. tricornutum* cultures (Figure 3A), consistent with those commonly reported [31]. The results showed that Chl *a* and Fuc were the two predominant pigments produced in *P. tricornutum*, which have previously been identified as the principal light harvesting pigments in *P. tricornutum* [21]. Over three weeks cultivation, the content of each pigment was found to decrease gradually in fusiform cell cultures but increase slightly in oval cell cultures. For example, on day 3, there were no significant differences in pigment content between fusiform and oval cell cultures of Pt1 8.6. However, after 21 days cultivation, the content of Chl *a*, Fuc, Diad, Chl *c*2 and  $\beta$ -car in fusiform cell cultures of Pt1 8.6 declined to 2.37, 2.20, 0.98, 0.33 and 0.06 mg g<sup>-1</sup> DW respectively, significantly lower than those from oval cell cultures of Pt1 8.6 which were 12.11, 12.03, 3.77, 1.99 and 0.55 mg g<sup>-1</sup> DW respectively. Pigments content in Pt4 cultures followed a similar trend (Figure 3A, lower panel).

This physiological response of declining pigment content in fusiform cell cultures with culture age is consistent with observations in *P. tricornutum* grown under nutrient deprivation. Specifically, high pigment was generally synthesised in actively growing microalgal cells under nutrient-replete conditions for efficient photosynthesis and cell division. When cells reached stationary phase accompanied with nutrient limitation, cell growth was inhibited and photosynthetic capacity was decreased. Furthermore, suppression of genes involved in photosynthesis and pigment biosynthesis in response to nitrogen and phosphorus deprivation has previously been observed in *P. tricornutum* [32, 33]. Thus, the low nutrient availability in f/2 medium could be responsible for the decreased pigment levels observed in fusiform *P. tricornutum* cultures.

By contrast, the M & M medium contains a relatively high nitrate and phosphate content, leading to the accumulation of pigment in oval cell cultures over time. The total pigment

content from oval cell cultures increased by more than 1.6-fold, from 1.90% DW to 3.04% DW in Pt1 8.6 and from 1.83% DW to 3.57% DW in Pt4 over 21 days cultivation. The observed dark brown color for oval cell cultures and yellow color for fusiform cell cultures (Figure S4) also revealed the higher pigment production from oval cells. In addition, the maximum fucoxanthin content was observed in oval cell cultures on day 21, reaching 12.0 mg g<sup>-1</sup> DW in Pt1 8.6 and 12.7 mg g<sup>-1</sup> DW in Pt4, corresponding to the highest volumetric concentrations of 8.5 mg L<sup>-1</sup> and 7.0 mg L<sup>-1</sup> respectively, which are more than 3.5-fold higher than those achieved in fusiform cell cultures (1.6 mg L<sup>-1</sup> in Pt1 8.6 and 2.0 mg L<sup>-1</sup> in Pt4). Our results confirmed the high content of fucoxanthin in *P. tricornutum*, and the fucoxanthin content obtained here in fusiform cell cultures is similar to those (2.1-5.5 mg g<sup>-1</sup> DW) reported in *P. tricornutum* grown in f/2 medium [34]. A higher content of 6-15.7 mg g<sup>-1</sup> DW was observed previously in *P. tricornutum* at a large scale of over 30 L depending on the nutrient conditions and extraction methods [5, 9]. Optimisation of cultivation time and scale-up parameters may enhance the pigment content obtained in oval cell cultures.

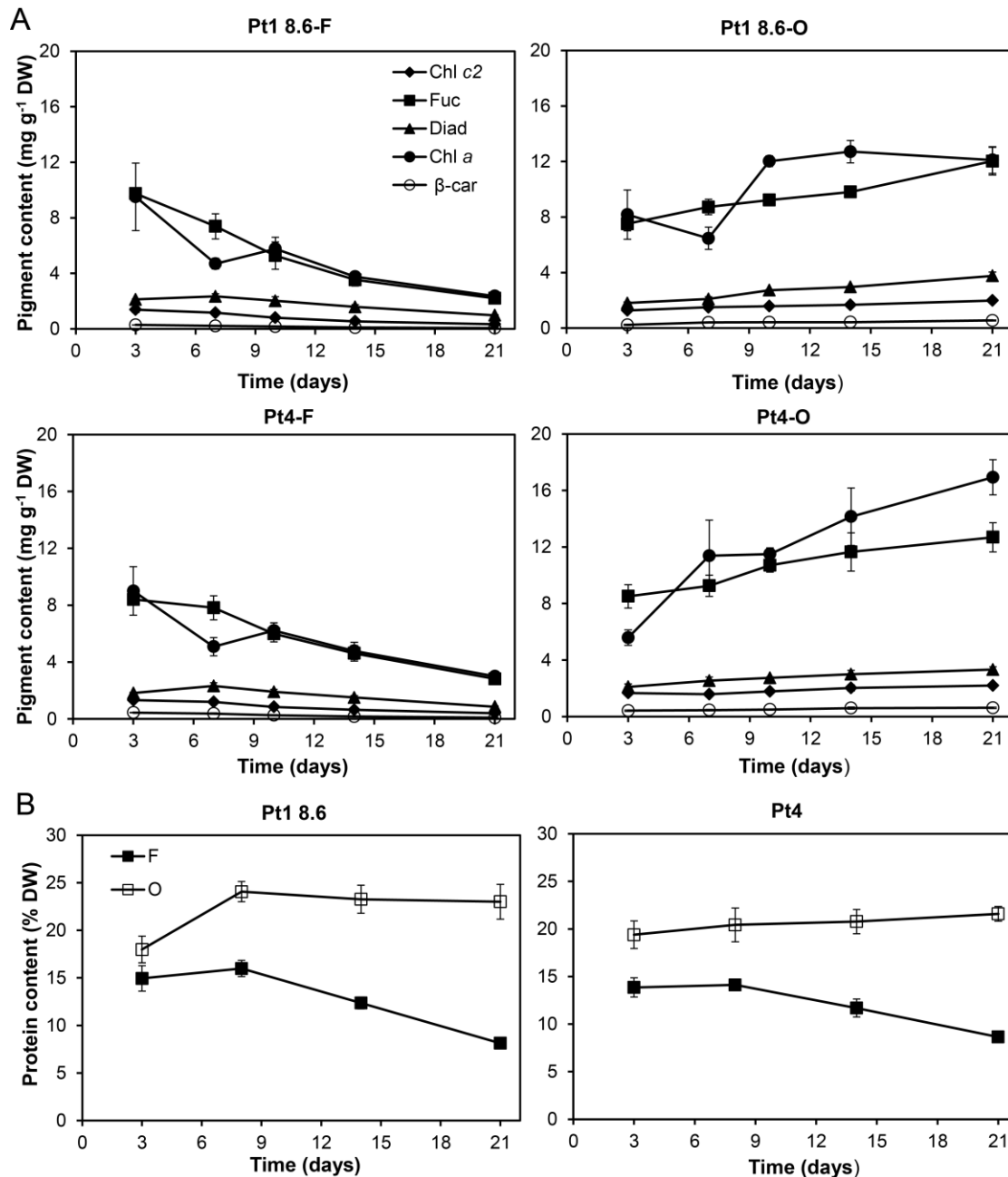


**Figure 3** Pigment and protein content in two morphotypes of *P. tricornutum* cells. (A) Quantification of five major pigments including chlorophyll *c2* (Chl *c2*), fucoxanthin (Fuc), diadinoxanthin (Diad), chlorophyll *a* (Chl *a*) and  $\beta$ -carotene ( $\beta$ -car) from fusiform (F) cell enriched cultures grown in f/2 medium or oval (O) cell enriched cultures grown in M & M medium in Pt1 8.6 and Pt4. (B) Total soluble protein content from fusiform (F) or oval (O) cell dominant cultures of Pt1 8.6 and Pt4. Data are shown as mean  $\pm$  one standard deviation from three biological replicates (n=3).

### 3.3.2 Protein content from fusiform and oval *P. tricornutum* cell cultures

The protein content (% DW) in the two morphotypes of cell cultures over cultivation time was investigated. Overall, higher protein content was obtained in oval cell cultures than in fusiform cell cultures for both strains at the time points tested (Figure 3B), implying the potential nutritional value of oval cells. Specifically, the protein content from oval cell cultures reached a plateau after experiencing an initial increase in the first 8 days cultivation, representing 24.06% DW in Pt1 8.6 and 20.43% DW in Pt4. By contrast, the protein content from fusiform cell cultures increased initially as well, reaching a maximum amount of 15.98% DW in Pt1 8.6 and 14.12% DW in Pt4 on day 8. After that, the values decreased gradually to 8.12% DW and 8.65% DW respectively by the end of cultivation.

In a study on Pt3, it was shown that 68% of the 2,326 differentially expressed genes were up-regulated and the nucleotide biosynthesis and protein processing were more active in oval cells, compared to fusiform and triradiate cells [35]. This may explain the higher protein content detected in oval cell cultures than in fusiform cell cultures even at the log phase of day 3 (Figure 3B). Highest protein content was observed at late log phase (~day 8), consistent with previous observations in microalgae [36]. Nutrient limitation, particularly nitrate and phosphate deprivation, in f/2 medium, as cultures reached stationary phase, is likely the main reason for the decrease in protein content observed in fusiform *P. tricornutum* cultures. This corroborates previous reports which have shown that genes involved in protein biosynthesis and folding were repressed and recycling of organic N resources such as protein, chlorophyll, nucleotide etc. was increased in *P. tricornutum* grown under nitrogen and phosphorus deprivation [32, 33].

### 3.3.3 Carbohydrate content from fusiform and oval *P. tricornutum* cell cultures

In order to improve the techno-economic feasibility of *Phaeodactylum* biorefinery, it is important to characterise the carbohydrates which can be converted to bioethanol or biobutanol. The polysaccharides from microalgae have also been shown to have some bioactivities such as antitumor, antibacterial, antioxidant, etc for potential pharmaceutical applications [37]. Thus, the carbohydrate content from the two morphotypes of *P. tricornutum* cultures were generally determined using the PSA assay, shown in line graphs in Figure 4. The cellular carbohydrate content in fusiform cell cultures showed a 3.5-fold change, rising from 10.17% DW to 35.73% DW in Pt1 8.6 and a 5.1-fold change, increasing from 9.88% DW to 50.72% DW in Pt4 over 21 days cultivation. However, no significant changes were observed in oval cell cultures, where the cellular carbohydrate content showed a plateau at approximately 21% DW in both strains. Since oval cells were known to secrete EPS [13], the released media-soluble polysaccharides were also investigated. It was found that oval cells produced more EPS than fusiform cells (2%-4% DW and 0.7%-2% DW, respectively). Our results showed that carbohydrate was accumulated in fusiform cells with the increasing culture age, in agreement with previous observations in this species and other microalgae [38, 39]. This could also be induced by the nutrient limitation in f/2 medium during log phase, which has been shown to redirect the photosynthetic carbon flow into N-deficient compounds, resulting in enhanced biosynthesis and accumulation in storage compounds like carbohydrates and lipids in microalgal cells [29, 40].

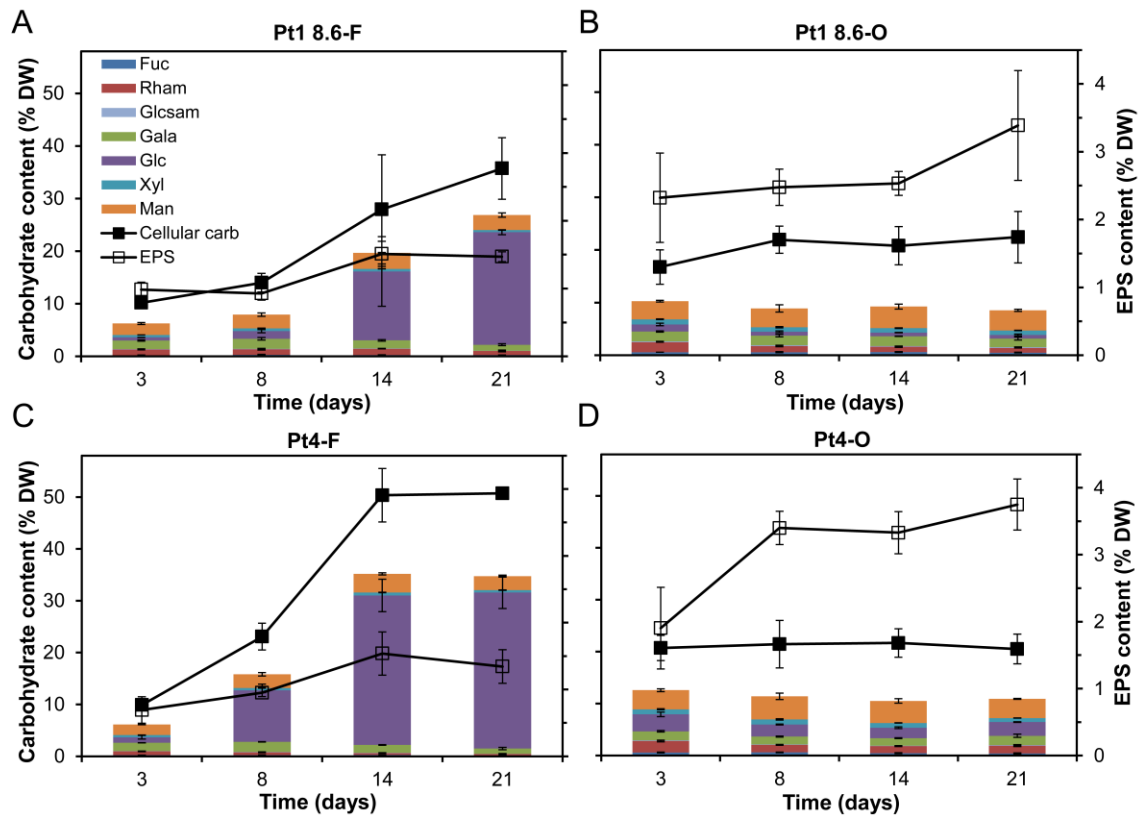


**Figure 4** Carbohydrate content and profile in two morphotypes of *P. tricornutum* cells. Line graphs show the cellular carbohydrate (Left axis) and EPS (Right axis) content determined by the PSA assay from fusiform (F) cell dominant cultures grown in f/2 medium (A, C) or oval (O) cell dominant cultures grown in M & M medium (B, D) in Pt1 8.6 and Pt4. Column bar charts indicate the cellular carbohydrate composition quantified by the HPLC method from fusiform (F) or oval (O) cell dominant cultures of Pt1 8.6 and Pt4. Fuc: fucose, Rham: rhamnose, Glcsam: glucosamine, Gala: galactose, Glc: glucose, Xyl: xylose and Man: mannose. Data are shown as mean  $\pm$  one standard deviation from three biological replicates (n=3).

An HPLC method was employed to further determine the cellular carbohydrate composition in order to quantify the easily-fermentable carbohydrates in *P. tricornutum* (Figure 4, column bar charts). The major monosaccharides detected in fusiform and oval cell cultures of Pt1 8.6 and Pt4 were shown to be fucose, rhamnose, glucosamine, galactose, glucose, xylose

and mannose, consistent with observations reported previously [26]. A similar trend of the rising total cellular carbohydrate content in fusiform cell cultures but stable levels in oval cell cultures over time was observed for both strains. However, the values obtained by the HPLC method are lower than those quantified from the PSA assay. This is most probably due to the glucose-equivalent quantification of total sugar in the PSA method which could overestimate carbohydrate content [26]. Another reason might be due to the omission of tiny unclassifiable peaks and other undetectable carbohydrates from the HPLC method causing underestimation of carbohydrate content.

Monosaccharide analysis demonstrated that the increase in cellular carbohydrate content from fusiform cell cultures resulted mainly from the accumulation of glucose, which constituted approximately 80% and 87% of total cellular carbohydrate in Pt1 8.6 and Pt4 respectively at the end of cultivation (Figure 4A&C). This observation is consistent with the known storage carbohydrate in the form of  $\beta$ -D-1,3-glucans, called chrysolaminarin in *P. tricornutum* [41]. Interestingly, the results also showed the higher amount of mannose and total cellular carbohydrate in oval cell cultures than in fusiform cell cultures on day 3. This is in agreement with previously observations of the activated biosynthesis of glucuronomannan, a main polysaccharide component of *P. tricornutum*'s cell wall [42], in oval cells in Pt3 [35].

#### **3.3.4 Lipid and fatty acid composition in fusiform and oval *P. tricornutum* cells**

In the context of lipid-based biodiesel production from microalgae, the neutral lipids stored as lipid bodies in two morphotypes of *P. tricornutum* cells were analysed qualitatively through BODIPY 505/515 cell staining. Representative images showed that with the increasing culture time, more and larger lipid bodies with stronger fluorescence intensity

were found in fusiform cells whereas no obvious formation of lipid bodies was observed in oval cells (Figure 5). This implies higher neutral lipid accumulation in fusiform cells than in oval cells over time. In agreement with the observations from BODIPY staining, FAME analysis showed that fusiform cells accumulated a high amount of lipid over time with the FAME-equivalent total fatty acids (TFAs) content increasing steadily from 6.71% DW to 22.93% DW in Pt1 8.6 and from 8.25% DW to 18.83% DW in Pt4 (Figure 6A&C). In contrast, there were no significant changes in TFAs content from oval cell cultures which stabilised at around 8% DW in Pt1 8.6 and 7% DW in Pt4 over 21 days cultivation (Figure 6B&D).

Microalgal lipid is composed of neutral lipids (NLs) and polar lipids (PLs). It is widely reported that NLs, primarily triacylglycerides (TAGs), were significantly accumulated while PLs were decreased upon nitrogen starvation in microalgae [29]. TAGs are precursors for biodiesel production [43] and PLs including glycolipids and phospholipids are important components of various cellular membrane structures [44]. Membrane lipid remodeling from phospholipids to nonphosphorus lipids followed by TAG accumulation was reported under phosphorus and nitrogen starvation in *P. tricornutum* [32, 33, 45]. Our results suggested that nitrogen and phosphorus deprivation was reached first in f/2 medium, inducing lipid accumulation in fusiform cells and the increase in TFAs content observed could largely be attributed to the increase in NLs.

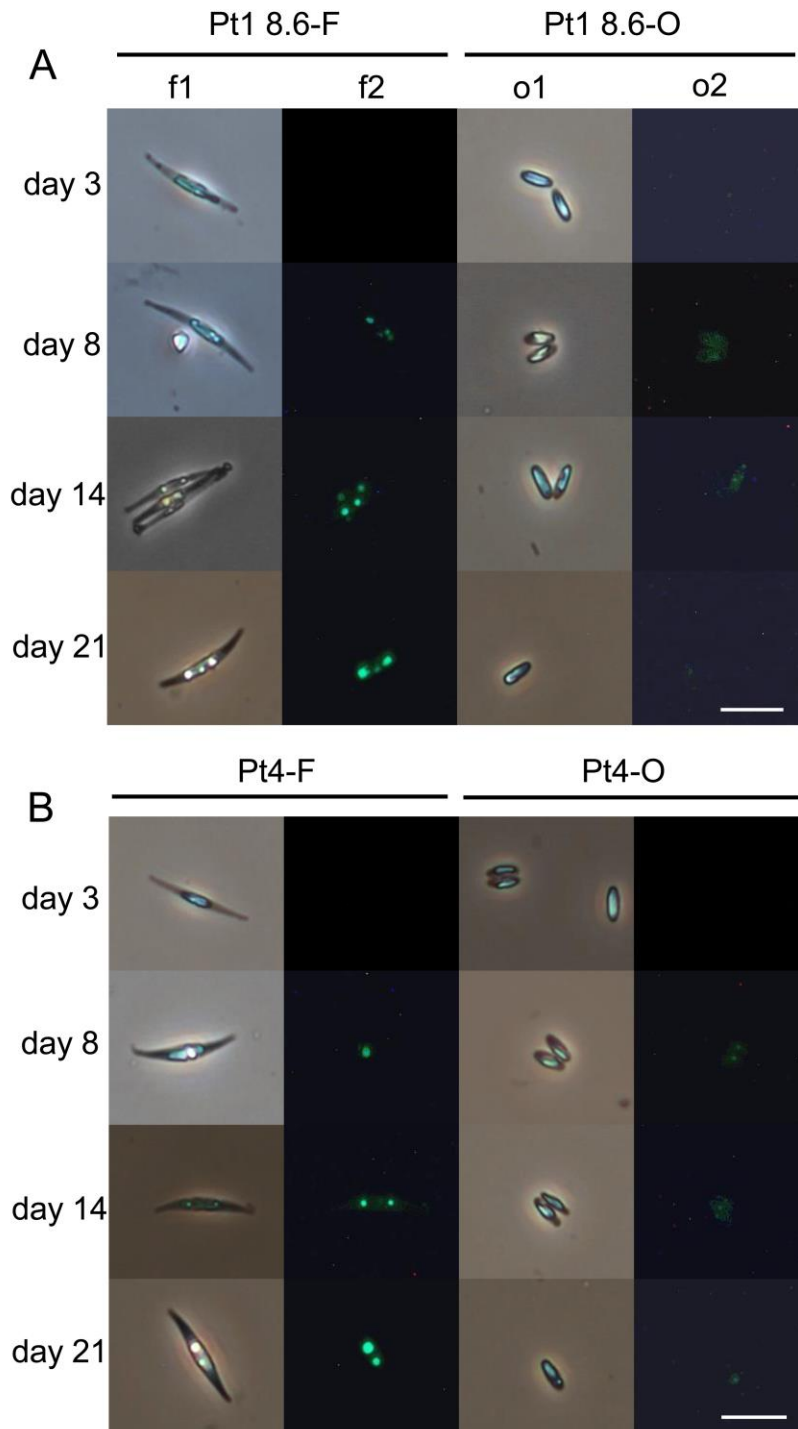


**Figure 5 Neutral lipid content in two morphotypes of *P. tricornutum* cells.** Micrographs showing the neutral lipid bodies formation over time in fusiform (F) and oval (O) cells of Pt1 8.6 (A) and Pt4 (B) stained with BODIPY 505/515. Lanes of f1 and o1 show the bright-field images of cells. Lanes of f2 and o2 are the corresponding fluorescent images. Scale bars: 20  $\mu\text{m}$ .

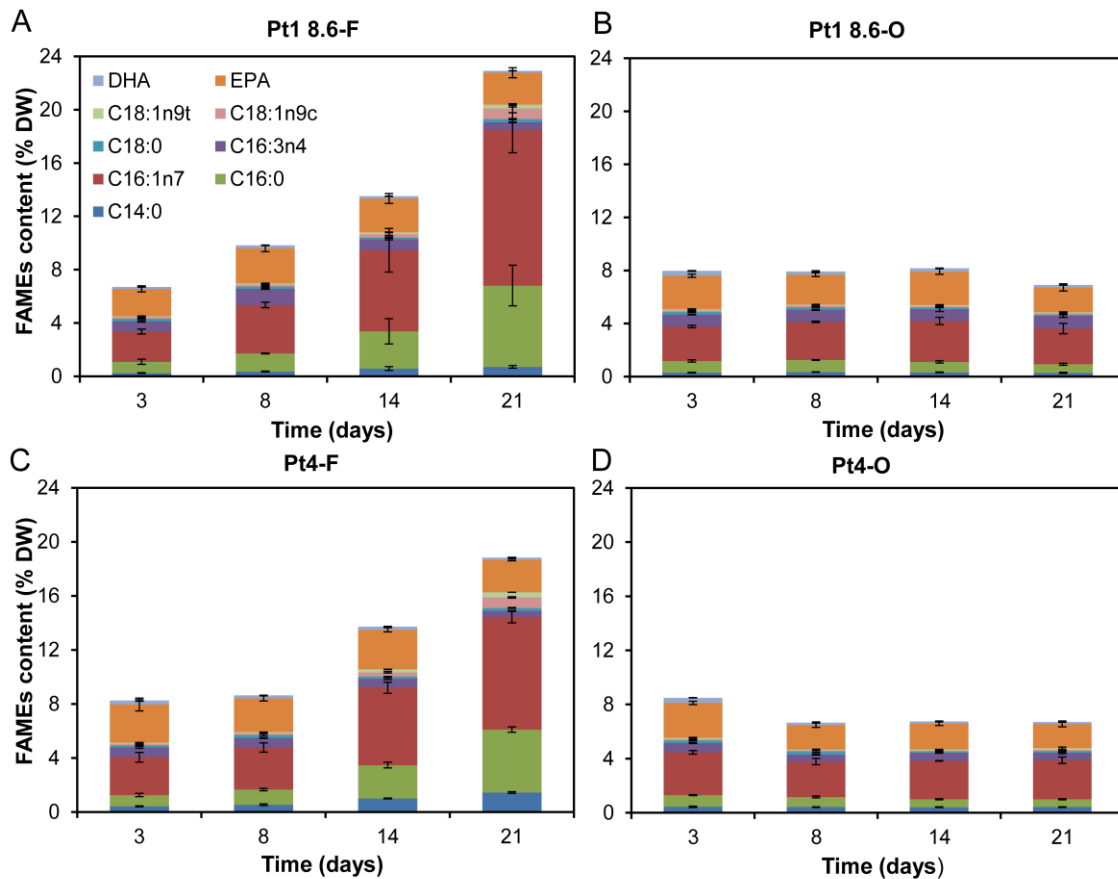


**Figure 6 Fatty acid composition and content in two morphotypes of *P. tricornutum* cells.**

Fatty acid composition and content quantified from fusiform (F) cell dominant cultures grown in f/2 medium (A, C) or oval (O) cell dominant cultures grown in M & M medium (B, D) in Pt1 8.6 and Pt4. Data are shown as mean  $\pm$  one standard deviation from three biological replicates (n=3).

The major fatty acids detected from fusiform and oval *P. tricornutum* cultures were found to be C<sub>14:0</sub>, C<sub>16:0</sub>, C<sub>16:1</sub>, C<sub>16:3</sub> and C<sub>20:5</sub> (EPA), plus small amount of C<sub>18</sub> families and C<sub>22:6</sub> (DHA) (Figure 6). A marked increase in the amount of C<sub>14:0</sub>, C<sub>16:0</sub>, C<sub>16:1</sub> and C<sub>18:1</sub> over the culture time was observed in fusiform cell cultures, leading to the rise in TFAs content. This outcome confirmed a general trend of increasing proportions of saturated fatty acids (SFAs) and monounsaturated fatty acids (MUFAs) but decreasing proportion of polyunsaturated fatty acids (PUFAs) over culture age [9, 29]. Fluorescent images showed the accumulation of NLS

in fusiform cells (Figure 5), implying that NLs consisted mainly of SFAs and MUFAs in *P. tricornutum*. By contrast, no significant change in the amount of each individual fatty acid was observed in oval cell cultures over the time studied. EPA was a major PUFA detected in both fusiform and oval *P. tricornutum* cultures (Figure 6). It is present in all lipid classes, but mainly in PLs and the highest EPA content was found in the glycolipid fraction of sulfoquinovosyl diacylglycerol (SQDG) [46]. *P. tricornutum* has been reported to contain about 1.7%-4.4% DW EPA depending on strains and growth conditions [47, 48]. Our results showed an EPA content of 2.0%-3.0% DW in fusiform cell cultures and 1.8%-2.6% DW in oval cell cultures with little changes observed over the cultivation period.

### **3.4 Overview on biomass profiles of fusiform and oval cells implying their industrial exploitation**

The profiles of total pigment, protein, carbohydrate and lipid from fusiform and oval *P. tricornutum* cultures over time were summarised (Table S3). From the perspective of industrial application, fusiform *P. tricornutum* cells maintained in f/2 medium were showed to be a potential feedstock for bioethanol and biodiesel production as carbohydrates and lipids were significantly accumulated in fusiform cell cultures with the increasing culture age (Figure 4, 5 & 6, Table S3). On the other hand, pigment, particularly fucoxanthin, was markedly accumulated in oval cell cultures grown in M & M medium, and higher protein (% DW) was obtained in oval cell cultures than in fusiform cell cultures over the cultivation period (Figure 3, Table S3). This indicates that oval *P. tricornutum* cells may be preferred for high pigment and protein production. Additionally, both fusiform and oval cells can be used for EPA production. Knowledge on biochemical composition in various cell morphotypes is essential for nutritional value evaluation and optimisation of *P. tricornutum* for industrial

biotechnology. By establishing the link between cell morphology and product accumulation over time, this work provides implications for the bioprocessing of this organism in terms of cultivation and harvest time. Our work also provides a reference for further improvement of overall biomass and classes of product yields from *P. tricornutum* and lays a foundation for deeper exploration on cell morphology control at genetic levels.

Harvest time is one of key parameters for optimal product yields. Here, the cultivation time was shown to have little effect on biomass composition in oval *P. tricornutum* cultures, which could be attributed to the high initial nutrient (11.76 mM nitrate and 0.57 mM phosphate) in M & M medium and implied the actively growing status of cells cultured in this medium under the conditions studied. However, from growth curves, early stationary phase seemed to be reached in oval *P. tricornutum* cultures after 21 days cultivation (Figure 2A). This suggested again that oval cell growth under this relatively high nutrient condition might be limited by other factors like carbon and light as inorganic carbon would become limited rapidly in relatively high light and high cell density conditions and the high cell density in flasks would cause self-shading. In contrast to our results, a more than 5-fold higher dry biomass concentration of 4.05 g L<sup>-1</sup>, a decrease in fucoxanthin content and an increase in total lipid content over time were observed in *P. tricornutum* grown under 14.5 mM nitrate and 0.88 mM phosphate at a large scale of 50 L aerated with 1% CO<sub>2</sub>-enriched air [9]. Further experiments such as an analysis of nutrient content remaining in culture media and optimisation of cultivation parameters would be helpful for understanding the morphological and biochemical responses of *P. tricornutum* to M & M medium and would also be important for scale-up bioprocess design.

#### **4. Conclusions**

This study offers a novel way to regulate cell morphology of *P. tricornutum* in liquid cultures. Stable cultures of Pt1 8.6 and Pt4 abundant with more than 90% oval cells were developed and well-maintained in M & M medium. Oval *P. tricornutum* cells were shown to be promising for high pigment and protein production while fusiform *P. tricornutum* cells were found to be a potential feedstock for biofuels production due to the marked accumulation of lipid and carbohydrate. By demonstrating the stability of oval morphotype in M & M medium, this work enables assessment of oval cells for potential industrial applications.

### **Acknowledgements**

The authors gratefully acknowledge the support from the Chinese Scholarship Council (stipend to Z.S.) and the Engineering and Physical Sciences Research Council Centre for Doctoral Training in Bioprocess Engineering Leadership [EP/L01520X/1].

### **Author contributions**

Author contributions to this work are listed as follows: conception and design of study (all authors), acquisition of data (Z.S.), analysis and interpretation of data (B.M.P. and Z.S.), drafting the manuscript (Z.S.), critical revision of the article for important intellectual content (B.M.P. and G.J.L.), and final approval of the version to be submitted (all authors). B.M.P. (brenda.parker@ucl.ac.uk) takes responsibility for the integrity of the work as a whole, from inception to finished article.

### **Statement of Informed Consent, Human/Animal Rights**

No conflicts, informed consent, or human or animal rights are applicable to this study.

### **Supplementary data**

Supplementary data of this work can be found in online version of this paper.

## References

- [1] C. Bowler, A.E. Allen, J.H. Badger, J. Grimwood, K. Jabbari, A. Kuo, U. Maheswari, C. Martens, F. Maumus, R.P. O'tillar, E. Rayko, A. Salamov, K. Vandepoele, B. Beszteri, A. Gruber, M. Heijde, M. Katinka, T. Mock, K. Valentin, F. Verret, J.A. Berges, C. Brownlee, J.P. Cadoret, A. Chiovitti, C.J. Choi, S. Coesel, A. De Martino, J.C. Detter, C. Durkin, A. Falciatore, J. Fournet, M. Haruta, M.J. Huysman, B.D. Jenkins, K. Jiroutova, R.E. Jorgensen, Y. Joubert, A. Kaplan, N. Kroger, P.G. Kroth, J. La Roche, E. Lindquist, M. Lommer, V. Martin-Jezequel, P.J. Lopez, S. Lucas, M. Mangogna, K. McGinnis, L.K. Medlin, A. Montsant, M.P. Oudot-Le Secq, C. Napoli, M. Obornik, M.S. Parker, J.L. Petit, B.M. Porcel, N. Poulsen, M. Robison, L. Rychlewski, T.A. Ryneerson, J. Schmutz, H. Shapiro, M. Siaut, M. Stanley, M.R. Sussman, A.R. Taylor, A. Vardi, P. von Dassow, W. Vyverman, A. Willis, L.S. Wyrwicz, D.S. Rokhsar, J. Weissenbach, E.V. Armbrust, B.R. Green, Y. Van de Peer, I.V. Grigoriev, The *Phaeodactylum* genome reveals the evolutionary history of diatom genomes, *Nature*, 456 (2008) 239-244.
- [2] U. Maheswari, T. Mock, E.V. Armbrust, C. Bowler, Update of the Diatom EST Database: a new tool for digital transcriptomics, *Nucleic acids research*, 37 (2009) D1001-1005.
- [3] E.B. Perez, I.C. Pina, L.P. Rodriguez, Kinetic model for growth of *Phaeodactylum tricornutum* in intensive culture photobioreactor, *Biochem Eng J*, 40 (2008) 520-525.
- [4] W. Yongmanitchai, O.P. Ward, Growth of and Omega-3-Fatty-Acid Production by *Phaeodactylum-Tricornutum* under Different Culture Conditions, *Appl Environ Microb*, 57 (1991) 419-425.
- [5] S.M. Kim, Y.J. Jung, O.N. Kwon, K.H. Cha, B.H. Um, D. Chung, C.H. Pan, A Potential Commercial Source of Fucoxanthin Extracted from the Microalga *Phaeodactylum tricornutum*, *Appl Biochem Biotech*, 166 (2012) 1843-1855.
- [6] S.C. Larsson, M. Kumlin, M. Ingelman-Sundberg, A. Wolk, Dietary long-chain n-3 fatty acids for the prevention of cancer: a review of potential mechanisms, *American Journal of Clinical Nutrition*, 79 (2004) 935-945.
- [7] T. Lebeau, J.M. Robert, Diatom cultivation and biotechnologically relevant products. Part II: Current and putative products, *Appl Microbiol Biot*, 60 (2003) 624-632.
- [8] J. Peng, J.P. Yuan, C.F. Wu, J.H. Wang, Fucoxanthin, a Marine Carotenoid Present in Brown Seaweeds and Diatoms: Metabolism and Bioactivities Relevant to Human Health, *Mar Drugs*, 9 (2011) 1806-1828.
- [9] B.Y. Gao, A.L. Chen, W.Y. Zhang, A.F. Li, C.W. Zhang, Co-production of lipids, eicosapentaenoic acid, fucoxanthin, and chrysolaminarin by *Phaeodactylum tricornutum* cultured in a flat-plate photobioreactor under varying nitrogen conditions, *J Ocean U China*, 16 (2017) 916-924.
- [10] D.P. Wilson, The triradiate and other forms of *Nitzschia closterium* (Ehrenberg) Wm. Smith, forma minutissima of Allen and Nelson, *J Mar Biol Assoc Uk*, 26 (1946) 235-270.
- [11] M.A. Borowitzka, B.E. Volcani, The Polymorphic Diatom *Phaeodactylum tricornutum*: Ultrastructure of Its Morphotypes<sup>1, 2</sup>, *J Phycol*, 14 (1978) 10-21.
- [12] A. De Martino, A. Bartual, A. Willis, A. Meichenin, B. Villazan, U. Maheswari, C. Bowler, Physiological and Molecular Evidence that Environmental Changes Elicit Morphological Interconversion in the Model Diatom *Phaeodactylum tricornutum*, *Protist*, 162 (2011) 462-481.
- [13] B. Tesson, C. Gaillard, V. Martin-Jezequel, Insights into the polymorphism of the diatom *Phaeodactylum tricornutum* Bohlin, *Bot Mar*, 52 (2009) 104-116.
- [14] A. De Martino, A. Meichenin, J. Shi, K.H. Pan, C. Bowler, Genetic and phenotypic characterization of *Phaeodactylum tricornutum* (Bacillariophyceae) accessions, *J Phycol*, 43 (2007) 992-1009.
- [15] H.A. Barker, Photosynthesis in diatoms, *Archives of Microbiology*, 6 (1935) 141-156.
- [16] S.A. Gutenbrunner, J. Thalhamer, A.M.M. Schmid, PROTEINACEOUS AND IMMUNOCHEMICAL DISTINCTIONS BETWEEN THE OVAL AND FUSIFORM MORPHOTYPES OF *PHAEODACTYLUM TRICORNUTUM* (BACILLARIOPHYCEAE) 1, *J Phycol*, 30 (1994) 129-136.
- [17] M. Herbstova, D. Bina, R. Kana, F. Vacha, R. Litvin, Red-light phenotype in a marine diatom involves a specialized oligomeric red-shifted antenna and altered cell morphology, *Sci Rep-Uk*, 7 (2017).
- [18] K.E. Cooksey, B. Cooksey, CALCIUM DEFICIENCY CAN INDUCE THE TRANSITION FROM OVAL TO FUSIFORM CELLS IN CULTURES OF *PHAEODACTYLUM TRICORNUTUM* BOHLIN1, 2, *J Phycol*, 10 (1974) 89-90.
- [19] A. Bartual, J.A. Gálvez, F. Ojeda, Phenotypic response of the diatom *Phaeodactylum tricornutum* Bohlin to experimental changes in the inorganic carbon system, *Bot Mar*, 51 (2008).

- [20] R.R. Guillard, Culture of phytoplankton for feeding marine invertebrates, Culture of marine invertebrate animals, Springer 1975, pp. 29-60.
- [21] J.E. Mann, J. Myers, On Pigments Growth and Photosynthesis of *Phaeodactylum Tricornutum*, J Phycol, 4 (1968) 349-8.
- [22] A. Silkina, K. Flynn, C. Llewellyn, C. Bayliss, Standard Operating Procedures for Analytical Methods and Data Collection in Support of Pilot-Scale Cultivation of Microalgae., Public Output report WP1A3.01 of the EnAlgae project, Swansea (2015) 395 pp.
- [23] S.W. Wright, S.W. Jeffrey, R.F.C. Mantoura, C.A. Llewellyn, T. Bjornland, D. Repeta, N. Welschmeyer, Improved Hplc Method for the Analysis of Chlorophylls and Carotenoids from Marine-Phytoplankton, Mar Ecol Prog Ser, 77 (1991) 183-196.
- [24] D.J. Smith, G.J.C. Underwood, The production of extracellular carbohydrates by estuarine benthic diatoms: The effects of growth phase and light and dark treatment, J Phycol, 36 (2000) 321-333.
- [25] M. Dubois, K.A. Gilles, J.K. Hamilton, P.A. Rebers, F. Smith, Colorimetric Method for Determination of Sugars and Related Substances, Anal Chem, 28 (1956) 350-356.
- [26] D.W. Templeton, M. Quinn, S. Van Wychen, D. Hyman, L.M.L. Laurens, Separation and quantification of microalgal carbohydrates, Journal of Chromatography A, 1270 (2012) 225-234.
- [27] M.S. Cooper, W.R. Hardin, T.W. Petersen, R.A. Cattolico, Visualizing "green oil" in live algal cells, J Biosci Bioeng, 109 (2010) 198-201.
- [28] F.G. Acien Fernandez, D.O. Hall, E. Canizares Guerrero, K. Krishna Rao, E. Molina Grima, Outdoor production of *Phaeodactylum tricornutum* biomass in a helical reactor, J Biotechnol, 103 (2003) 137-152.
- [29] G. Breuer, P.P. Lamers, D.E. Martens, R.B. Draaisma, R.H. Wijffels, The impact of nitrogen starvation on the dynamics of triacylglycerol accumulation in nine microalgae strains, Bioresource Technol, 124 (2012) 217-226.
- [30] C.J.A. Ridley, B.M. Parker, L. Norman, B. Schlarb-Ridley, R. Dennis, A.E. Jamieson, D. Clark, S.C. Skill, A.G. Smith, M.P. Davey, Growth of microalgae using nitrate-rich brine wash from the water industry, Algal Res, 33 (2018) 91-98.
- [31] N. Domingues, A.R. Matos, J. Marques da Silva, P. Cartaxana, Response of the diatom *Phaeodactylum tricornutum* to photooxidative stress resulting from high light exposure, Plos One, 7 (2012) e38162.
- [32] L. Alipanah, J. Rohloff, P. Winge, A.M. Bones, T. Brembu, Whole-cell response to nitrogen deprivation in the diatom *Phaeodactylum tricornutum*, J Exp Bot, 66 (2015) 6281-6296.
- [33] L. Alipanah, P. Winge, J. Rohloff, J. Najafi, T. Brembu, A.M. Bones, Molecular adaptations to phosphorus deprivation and comparison with nitrogen deprivation responses in the diatom *Phaeodactylum tricornutum*, Plos One, 13 (2018) e0193335.
- [34] H. Wu, T. Li, G. Wang, S. Dai, H. He, W. Xiang, A comparative analysis of fatty acid composition and fucoxanthin content in six *Phaeodactylum tricornutum* strains from different origins, Chinese journal of oceanology and limnology, 34 (2016) 391-398.
- [35] C. Ovide, M.-C. Kiefer-Meyer, C. Bérard, N. Vergne, T. Lecroq, C. Plasson, C. Burel, S. Bernard, A. Driouich, P. Lerouge, Comparative in depth RNA sequencing of *P. tricornutum*'s morphotypes reveals specific features of the oval morphotype, Sci Rep-Uk, 8 (2018) 14340.
- [36] C.M. Gatenby, D.M. Orcutt, D.A. Kreeger, B.C. Parker, V.A. Jones, R.J. Neves, Biochemical composition of three algal species proposed as food for captive freshwater mussels, J Appl Phycol, 15 (2003) 1-11.
- [37] S.F. Yang, H.T. Wan, R. Wang, D.J. Hao, Sulfated polysaccharides from *Phaeodactylum tricornutum*: isolation, structural characteristics, and inhibiting HepG2 growth activity in vitro, Peerj, 7 (2019).
- [38] Y. Liang, J. Beardall, P. Heraud, Changes in growth, chlorophyll fluorescence and fatty acid composition with culture age in batch cultures of *Phaeodactylum tricornutum* and *Chaetoceros muelleri* (Bacillariophyceae), Bot Mar, 49 (2006) 165-173.
- [39] S.H. Ho, S.W. Huang, C.Y. Chen, T. Hasunuma, A. Kondo, J.S. Chang, Characterization and optimization of carbohydrate production from an indigenous microalga *Chlorella vulgaris* FSP-E, Bioresource Technol, 135 (2013) 157-165.
- [40] I. Pancha, K. Chokshi, B. George, T. Ghosh, C. Paliwal, R. Maurya, S. Mishra, Nitrogen stress triggered biochemical and morphological changes in the microalgae *Scenedesmus* sp CCNM 1077, Bioresource Technol, 156 (2014) 146-154.
- [41] C.W. Ford, E. Percival, 1298. The carbohydrates of *phaeodactylum tricornutum*. Part I. Preliminary examination of the organism, and characterisation of low molecular weight material and of a glucan, Journal of the Chemical Society (Resumed), (1965) 7035-7041.
- [42] T. Le Costaouec, C. Unamunzaga, L. Mantecon, W. Helbert, New structural insights into the cell-wall polysaccharide of the diatom *Phaeodactylum tricornutum*, Algal Res, 26 (2017) 172-179.
- [43] Y. Chisti, Biodiesel from microalgae, Biotechnology advances, 25 (2007) 294-306.

- [44] G. van Meer, D.R. Voelker, G.W. Feigenson, Membrane lipids: where they are and how they behave, *Nat Rev Mol Cell Bio*, 9 (2008) 112-124.
- [45] H. Abida, L.J. Dolch, C. Mei, V. Villanova, M. Conte, M.A. Block, G. Finazzi, O. Bastien, L. Tirichine, C. Bowler, F. Rebeille, D. Petroustos, J. Jouhet, E. Marechal, Membrane glycerolipid remodeling triggered by nitrogen and phosphorus starvation in *Phaeodactylum tricornutum*, *Plant Physiol*, 167 (2015) 118-136.
- [46] Y.H. Yang, L. Du, M. Hosokawa, K. Miyashita, Y. Kokubun, H. Arai, H. Taroda, Fatty Acid and Lipid Class Composition of the Microalga *Phaeodactylum tricornutum*, *J Oleo Sci*, 66 (2017) 363-368.
- [47] A.R. Medina, E.M. Grima, A.G. Gimenez, M.J.I. Gonzalez, Downstream processing of algal polyunsaturated fatty acids, *Biotechnology advances*, 16 (1998) 517-580.
- [48] P. Steinrucken, S.K. Prestegard, J.H. de Vree, J.E. Storesund, B. Pree, S.A. Mjos, S.R. Erga, Comparing EPA production and fatty acid profiles of three *Phaeodactylum tricornutum* strains under western Norwegian climate conditions, *Algal Res*, 30 (2018) 11-22.